Astron. Astrophys. 341, 418–426 (1999)

ASTRONOMY AND ASTROPHYSICS

8.4 GHz VLBI monitoring of the gamma-bright blazar PKS 0528+134

S. Britzen[1,2], **A. Witzel**[1], **T.P. Krichbaum**[1], **S.J. Qian**[1,3], **and R.M. Campbell**[2]

[1] Max-Planck-Institut für Radioastronomie, Auf dem Hügel 69, D-53121 Bonn, Germany
[2] Netherlands Foundation for Research in Astronomy, 7991 PD Dwingeloo, The Netherlands
[3] Beijing Astronomical Observatory, Chinese Academy of Sciences, Beijing 10080, P.R. China

Received 7 July 1998 / Accepted 17 August 1998

Abstract. We present an analysis of the structural evolution of the jet of PKS 0528+134, one of the strongest gamma-active blazars. We study almost eight years (1986.25 – 1994.07) of jet evolution using 20 epochs taken from the extensive database of X-band geodetic VLBI observations. We discuss the activity and kinematics of the jet in the light of the prominence of this source in the high energy regime. Rapid structural changes take place in its jet, and the VLBI image undergoes obvious structural evolution across the epochs in which the component motion follows different bent paths. The simplest model portrays PKS 0528+134 as a bent jet of length $\sim 5-6$ mas comprising seven jet features. Not unexpectedly for a gamma-active quasar, we find superluminal motion of $\sim 4-6c$ for five of the jet components. These five jet features can be traced over the entire observing period, while two newer components were ejected at times near epochs of enhanced gamma-ray activity. We can associate the increased activity in the radio and gamma-ray bands with morphological changes in the source structure. We discuss the possible link between curvature of the jet and the brightness of the source at high energies.

Key words: galaxies: jets – galaxies: quasars: general – radio continuum: galaxies – gamma rays: theory

1. Introduction

The EGRET detector on board the *Compton Gamma Ray Observatory* (CGRO) has detected 51 active galactic nuclei (AGNs) with energy E > 100 MeV (Thompson et al. 1995; Fichtel et al. 1994; Sreekumar et al. 1996; von Montigny et al. 1995). Most of these sources show rapid luminosity variations (with the smallest timescale as short as a few hours [Wagner, private communication]), are compact, and are radio-loud, flat-spectrum blazars. Among the EGRET-detected sources, PKS 0528+134 is especially noteworthy due to its enormous brightness and its degree of variability at high energies (Hunter et al. 1993, Mukherjee et al. 1996).

Over a span of almost 8 years, frequent VLBI observations of this source have been conducted, and these allow us to study phenomena characteristic of gamma-ray blazars: e.g., evidence has been presented for some sources that component ejections and outbursts in the high-energy range are correlated. However, the question concerning the temporal sequence of these phenomena remains unanswerable due to insufficient data. Our data offer the opportunity for the first time to study this relation in detail and to correlate jet components with specific flares. Our frequent observations allow us to analyze the jet activity and its connection to broad-band flux-density variability. PKS 0528+134 showed significant outbursts in the hard gamma-ray regime in 1991 (Sreekumar et al. 1993), and again at a level approximately three times greater during 1993 March 23-29. As one of the gamma-ray detected sources, it shows gamma-ray variability on timescales of a few days (Mukherjee et al. 1996). The *Oriented Scintillation Spectrometer Experiment* (OSSE) detected PKS 0528+134 and found variability in the energy band 50-150 keV (McNaron-Brown et al. 1995). PKS 0528+134 has been identified as a low-polarized quasar in the optical wavebands (Fugmann & Meisenheimer 1988), with B=20.0 (Condon et al. 1977), V=19.5 (Wall & Peacock 1985), and z=2.07 (Hunter et al. 1993).

The radio spectrum was flat with a spectral index of 0.47 between 2.7 and 5 GHz at the epoch of the 1 Jy catalogue (Kühr et al. 1981). PKS 0528+134 is also known for its pronounced flux-density variability in the radio regime (Aller et al. 1985; Aller & Aller 1996; Zhang et al. 1994; Valtaoja & Teraesranta 1995, 1996; Stevens et al. 1994; Reich et al. 1993; Pohl et al. 1995, 1996). Multifrequency radio observations have been performed (Reich et al. 1993; Pohl et al. 1995, 1996); these suggest correlated variability across the radio part of the spectrum with a delay at lower frequencies. The first VLBI maps of PKS 0528+134 (Charlot 1990), which were limited in dynamic range, show a one-sided extension at 2.3 GHz and a double structure at 8.4 GHz. Zhang et al. (1994) presented VLBI data obtained at 8 and 22 GHz, and discussed a possible two-sidedness of the source structure. They investigated a possible correlation between changes in the source's spectrum and structure in the context of a synchrotron self-Compton (SSC) analysis. Pohl et al. (1995) presented a revised component identification based on VLBI observations at 8.4 and 22 Ghz; superluminal motion was verified for two jet components ($v \sim 4.4\ c$). This paper also presented the detection of a new jet component after a major radio flare. Krichbaum et al. (1995) reported VLBI obser-

Send offprint requests to: S. Britzen (sbritzen@nfra.nl)

vations, including observations at higher frequencies (8, 22, 43 and 86 GHz), that suggested at least three moving (at apparent velocities $\beta_{\rm app} \simeq 5$) and two apparently stationary jet components. They presented correlations among component-ejection, flux-density activity in the mm-bands, and a preceding intense flare of the gamma-flux density observed in early 1993. Until recently, no systematic study of the morphological changes in PKS 0528+134 has been published. All previously mentioned observations suffer from insufficient time coverage. Observations from the geodetic database allow a more detailed analysis of the kinematics and an investigation of a possible correlation with gamma-activity.

In the following we will focus on the VLBI observations, discuss the component identification and the resultant superluminal motion, present an analysis of component trajectories, and question the correlation between gamma-ray activity and morphological variability in the radio. Results have previously appeared, e.g., Krichbaum et al. (1995, 1998) and Britzen et al. (1996, 1997, 1998). We use the following parameters for the calculations throughout the paper: $H_0 = 100$ km s^{-1} Mpc^{-1} and $q_0 = 0.5$.

2. VLBI observations and data analysis

2.1. Geodetic VLBI

The geodetic database provides a unique tool to follow the kinematics of compact extragalactic objects over a time span of $\sim$ 15 years with time sampling as high as 12 epochs per year in some cases. The principal aim of the observations, however, has been the determination of station coordinates by snapshot observations of 15-20 sources in a single experiment. Despite the limited uv-coverage in a single experiment, averaging over the image structure across the epochs effectively downweights morphological features that are insufficiently constrained at any given epoch. Previous papers have reported on the astronomical investigation of geodetic VLBI data, and have presented maps and model-fits (Charlot 1990, 1992; Tang 1987, 1988, 1989; Schalinski 1988; Vicente 1996; Piner & Kingham 1997). In this paper we concentrate on the detailed analysis of only one source, but with high temporal resolution. An advantage of using archived geodetic observations is that for the observed sources, we can obtain a dense sampling in time - of particular value for such application as mapping the evolution of the jet as we do for PKS 0528+134 - albiet that the individual images may not be of high quality. Our data were taken from the geodetic archive at the Mark III correlator of the Max-Planck-Institut für Radioastronomie in Bonn. We preferentially investigated IRIS- and IRIS-S observations (International Radio Interferometric Surveying, S=South; Carter & Robertson 1984; Carter et al. 1988). Usually 3- to 6-station VLBI arrays participate in IRIS-S observations providing a resolution of ~ 0.5 mas. In a usual observing run, about fifteen sources, almost equally distributed in the sky, are observed between ten and fifteen times for about three to seven minutes each during 24 hours of observation. The data are recorded simultaneously at 2.3 and 8.4 GHz in the MK III recording format.

Table 1. The table lists the geodetic VLBI campaigns whose observations were used in this paper. Column 1 denotes the name of the experiment, column 2 the date of the observation, column 3 the antennas, and column 4 the number of scans performed on PKS 0528+134. This serves as a crude measure of the uv-coverage. Abbreviations have been used for the participating telescopes, see Table 2.

Exp.	Epoch	Stations	$N_{\rm scans}$
IRIS316	1986.25	HR-O-R-WS-WT	180
IRIS359	1986.84	HR-O-R-WS-WT	168
IRIS422	1987.71	HR-O-R-WS-WT	173
IRIS468	1988.33	HR-O-WS-WT	112
IRIS513	1988.95	HR-R-WS-WT	169
IRIS540	1989.32	HR-O-R-WS-WT	187
IRIS-S30	1990.38	HA-M-R-WS-WT	240
IRIS-S39	1991.12	HA-M-R-WS-WT	168
IRIS-S40	1991.23	HA-M-R-WS-WT	255
IRIS-S41	1991.31	HA-M-N-R-WS-WT	144
IRIS-S42	1991.34	HA-M-N-R-WS-WT	200
IRIS-S43	1991.44	HA-M-N-R-WS-WT	136
IRIS-S48	1991.86	HA-M-N-R-WS-WT	129
IRIS-S51	1992.15	HA-M-N-R-WS-WT	129
IRIS-S52	1992.19	HA-M-N-R-WS-WT	80
IRIS-S63	1993.11	HA-SA-WS-WT	152
IRIS-S65	1993.30	HA-FO-SA-WS-WT	166
IRIS-S68	1993.53	HA-FO-SA-WS-WT	322
IRIS-S72	1993.84	HA-FO-WS-WT	176
IRIS-S74	1994.07	HA-FO-WS-WT	163

Table 2. Station abbreviations used in Table 1

Abbs.	Station	Country	Diameter [m]
D	DSN-Madrid	Spain	34
F	Fortalezza	Brazil	22
HA	Hartebeesthoek	South Africa	26
HR	Fort Davis	USA	25
M	Mojave	USA	12
N	Noto	Italy	32
O	Onsala	Sweden	20
R	Richmond	USA	18
WS	Westford	USA	18
WT	Wettzell	Germany	20

2.2. VLBI observations of PKS 0528+134

PKS 0528+134 has been included in regular geodetic monitoring for more than ten years, and more than 100 individual observations have been obtained. From the total of all IRIS & IRIS-S VLBI observations of PKS 0528+134, we selected the 20 X-band data sets with at least 4 antennas participating. A second factor in the selection of the datasets was the desire to obtain an almost uniform temporal distribution of observations over the eight-year period from 1986.25 to 1994.07. Tables 1 and 2 summarize details concerning the observations. We transferred the data, after export from the correlator, into the Caltech VLBI-package and calibrated them with the standard technique using system temperatures and antenna sensitivities (e.g., Cohen

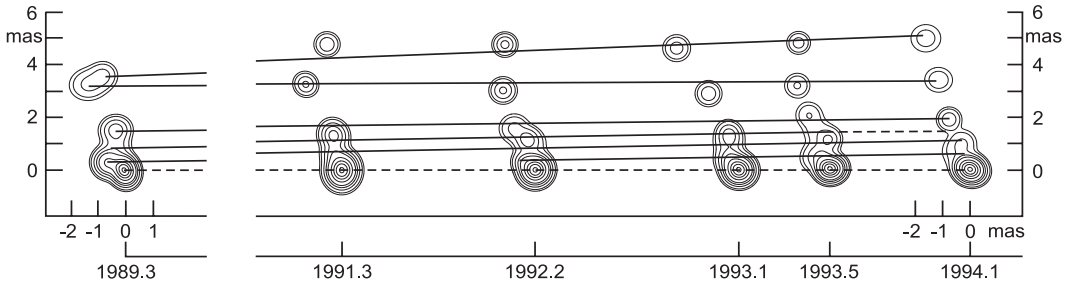

Fig. 1. Mosaic plot of six selected epochs, illustrating the structure of PKS 0528+134 and the motion of the individual components. The lines correspond to a linear fit to these motions, as illustrated in more detail in Fig. 2.

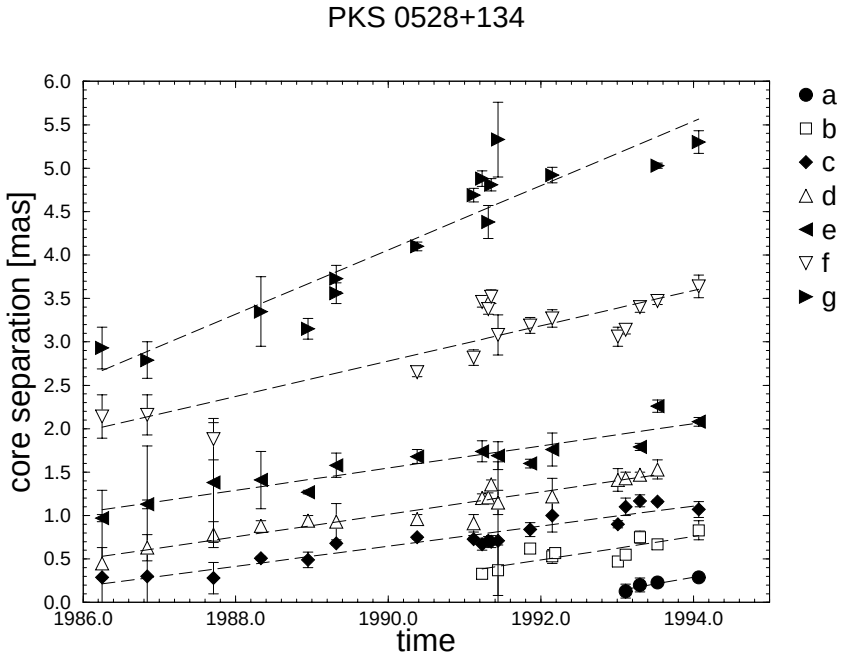

Fig. 2. The inner 7 components of PKS 0528+134 and their kinematics between 1986 and 1994.

1975). We used the two sources 1803+784 and 4C39.25 to check the accuracy of the amplitude- and phase calibration because of their well-known VLBI structure and brightness. The morphologies of these two sources have been monitored within independent astronomical observations at various wavelengths (see, e.g., Marcaide et al. 1989 and Alberdi et al. 1993 for 4C39.25; Eckart et al. 1986 and Witzel et al. 1988 for 1803+784). We scaled the flux densities using single-dish measurements from the Michigan Radio Telescope that were kindly provided by H. Aller and M. Aller. We performed the imaging with the standard procedures provided in the Caltech VLBI-package. Starting from a point-source model, we mapped the source using the CLEAN algorithm. In order to quantify the source structure, we also fitted elliptical Gaussian components to the observed visibilitites at each epoch. Depending on data quality and uv-coverage we were able to fit models comprising typically 5–8 Gaussian components. We determined the errors of the individual parameters using formal error propagation in the least-square fits (program ERRFIT in the CIT-package). From previous experience with geodetic data analysis, we realized that the errors calculated with ERRFIT may not be realistic for these kinds of datasets. The following errors reflect systematic effects in the elliptical Gaussian models: $\Delta S \sim$ 10-20%, $\Delta r \sim$ 0.1 mas, $\Delta\Theta \sim 20^\circ - 30^\circ$ for $r < 0.5$ mas, and $\Delta\Theta \sim 5^\circ - 10^\circ$ for $r >$0.5 mas. Table 3 gives the results of the model-fitting procedure.

3. Results

3.1. Overall morphology

In Fig. 1 we show the structural evolution of the inner VLBI jet of PKS 0528+134. For the time range from 1989.32 to 1994.07, we plot individual maps of the Gaussian model fits. The overall source structure shows a one-sided northerly bent jet, which agrees well with the structure seen earlier by Pohl et al. (1995) and Krichbaum et al. (1995, 1998). The bending appears more pronounced near the core ($r \leq 1.5$ mas) than further away. Within the inner $\sim$ 1.5 mas, the jet appears to bend twice, the first time within the inner $\sim$ 0.5 mas and the second beyond $\sim$ 1 mas. Our data yield no evidence for a possible counterjet, as postulated by Zhang et al. (1994). In the following, we therefore assume the brightest and most compact VLBI component, located at the southern end of the jet, is the core. This identification is consistent with the core identified by Pohl et al.

Table 3. Model-fit results for PKS 0528+134. As discussed in the text we take $\Delta S \sim$ 10-20%, $\Delta r \sim 0.1$ mas, $\Delta\Theta \sim 20^\circ - 30^\circ$ for $r < 0.5$ mas, and $\Delta\Theta \sim 5^\circ - 10^\circ$ for $r >$0.5 mas.

Epoch	Component	S [Jy]	r [mas]	θ [deg]
1986.25	k	3.4	.0	.0
	c	.1	.3	187
	d	.1	.5	128
	e	.5	1.0	56
	f	.1	2.1	5
	g	.1	2.9	19
	x	.1	4.8	9
1986.84	k	2.0	.0	.0
	c	.1	.3	182
	d	.1	.6	128
	e	.1	1.1	105
	f	.1	2.2	7
	g	.1	2.8	8
1987.71	k	1.1	.0	.0
	c	.4	.3	189
	e	.5	1.4	60
	f	.5	1.9	7
	d	.1	.8	114
1988.33	k	.8	.0	.0
	c	.7	.5	106
	d	.4	.9	34
	e	.1	1.4	31
	g	.1	3.4	−1
	x	.1	5.9	3
1988.95	k	.5	.0	.0
	c	.1	.5	81
	d	.1	.9	32
	e	.7	1.3	34
	g	.1	3.2	18
	x	.1	5.1	10
1989.32	k	1.2	.0	.0
	c	.5	.7	65
	d	.1	.9	18
	e	.2	1.6	11
	g	.2	3.6	22
	g	.1	3.7	12
1990.38	k	1.1	.0	.0
	c	.1	.8	40
	d	.1	1.0	5
	e	.1	1.7	17
	f	.1	2.7	1
	g	.2	4.1	12
	x	.3	5.3	1
1991.12	k	1.4	.0	.0
	c	.2	.7	40
	d	.1	.9	4
	f	.1	2.8	5
	g	.1	4.7	2
1991.23	k	.7	.0	.0
	b	.2	.3	57
	c	.3	.7	25
	d	.1	1.2	22
	e	.1	1.7	18
	f	.1	3.5	24
	g	.1	4.9	7
1991.31	k	1.0	.0	.0
	c	.3	.7	17
	d	.1	1.2	17
	f	.1	3.4	18
	g	.1	4.4	1
1991.35	k	1.2	.0	.0
	c	.1	.7	24
	d	.2	1.4	13
	f	.1	3.5	22
	g	.1	4.8	7
1991.44	k	.9	.0	.0
	b	.1	.4	54
	c	.1	.7	18
	d	.1	1.2	20
	e	.1	1.7	22
	f	.1	3.1	2
	g	.2	5.3	4
1991.86	k	1.1	.0	.0
	b	.1	.6	49
	c	.1	.8	18
	e	.1	1.6	14
	f	.1	3.2	23
	x	.1	4.7	26
1992.15	k	1.2	.0	.0
	b	.1	.5	53
	c	.1	1.0	11
	d	.1	1.2	14
	e	.1	1.8	26
	f	.1	3.3	22
	g	.1	4.9	13
1992.19	k	1.2	.0	.0
	b	.1	.6	32
	x	.1	.9	39
1993.01	k	1.1	.0	.0
	b	.1	.5	37
	d	.1	1.4	15
	f	.1	3.1	20
	c	.1	.9	11
1993.11	k	1.2	.0	.0
	a	.1	.1	66
	b	.2	.6	40
	c	.1	1.1	20
	d	.1	1.4	15
	f	.1	3.1	21
	x	.1	5.2	26
1993.30	k	1.9	.0	.0
	a	.1	.2	70
	b	.2	.8	46
	c	.1	1.2	27
	d	.1	1.5	13
	e	.1	1.8	18
	x	.2	3.4	39
	f	.2	3.4	21
1993.53	k	1.1	.0	.0
	a	.4	.2	65
	b	.3	.7	43
	c	.1	1.2	5
	d	.1	1.5	20
	e	.1	2.3	22
	f	.1	3.5	22
	g	.1	5.0	14
1994.07	k	1.6	.0	.0
	a	.1	.3	61
	b	.1	.8	37
	c	.1	1.1	16
	e	.1	2.1	22
	f	.1	3.6	19
	g	.1	5.3	18

(1995). Our core identification is further supported by the fact that all secondary jet components seem to move away from it. It shows pronounced flux density variability, and it has an inverted spectrum. Letters **a**–**g** denote individual components found in the model fits, see Table 3. In Fig. 1 we also plot straight lines to indicate individual components and their motions. Inspection of all data sets yields strong evidence for at least seven distinct jet components within ∼5 mas of the core. The outer five components (**c**, **d**, **e**, **f**, and **g**) can be traced through the full eight years, while the two innermost components (**a** and **b**) were ejected more recently; see Fig. 2. There we plot the separations of the components **a**–**g** from the core as a function of time. We derived linear estimates on the motions of the individual components by fitting straight lines to these points. The components that lie within the inner two milliarcseconds all move with a similar velocity of $\beta_{app} \simeq 5$. Table 4 summarizes the results of these fits. Components **f** and **g**, which lie further out, show higher separation velocities from the core and are not included

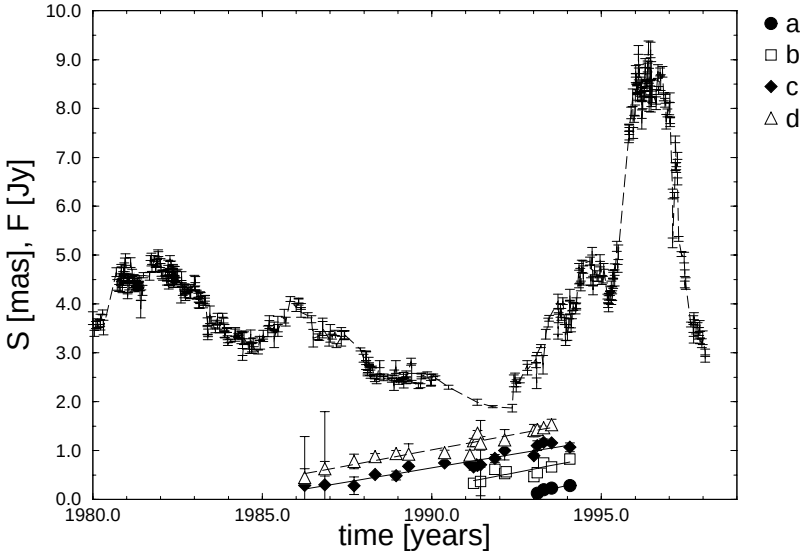

Fig. 3. Flux-density evolution at 8 GHz superimposed on the motion of the four youngest jet components in PKS 0528+134 (S: separation from the core; F: flux density).

Table 4. Component velocities calculated assuming linear outward motion for the components within ~ 2 mas from the core.

Ident.	$\mu \pm \Delta\mu$[mas/year]	$\beta_{app} \pm \Delta\beta_{app}$	$t_0 \pm \Delta t_0$
a	0.15 ± 0.03	6.2 ± 1.3	1992.1 ± 0.4
b	0.14 ± 0.03	5.5 ± 1.4	1988.4 ± 1.0
c	0.12 ± 0.01	4.7 ± 0.4	1984.4 ± 2.3
d	0.13 ± 0.01	5.2 ± 0.4	1982.1 ± 2.3
e	0.13 ± 0.01	5.2 ± 0.6	1977.9 ± 2.5

in Table 4. We extend this simplistic picture of PKS 0528+134 in Sect. 3.3 by investigating curvature in the paths of individual components.

3.2. Component ejection and flux-density variability

Extrapolation of the components' motion backwards in time allows us to investigate the relation between their ejections and the total flux-density activity. Table 4 also lists the time of ejection from the core, t_0, for the jet components within ~ 2 mas from the core, as extrapolated from the linear separation velocity. Within the accuracy of this "back-extrapolation", which is somewhat limited by any unmodelled accelerations at small separations, it appears that the ejection times of these components can be related to the beginning of a period of enhanced variation in the flux-density at 8 GHz, which we show in Fig. 3. There we show a 8 GHz light-curve from the Michigan monitoring data and the separation from the core, $r(t)$, for the inner four components **a**–**d**. Whereas the pair of the older components **c** and **d** could be related to the maximum in the light-curve near 1986, the pair of the younger components **a** and **b** relates to the beginning of two secondary outbursts peaking in $\sim$ 1993.6 and $\sim$ 1994.6. We note that these secondary flares were accompanied by a major outburst in the gamma-regime which peaked in March 1993 (Mukherjee et al. 1996). From high-frequency VLBI observations, Krichbaum et al. (1995) reported the ejection of a new jet component near the time of the gamma-flare. It is therefore very tempting to identify our component **a** with their component **N2**. Small differences in the positions of these components relative to the core could be attributed to frequency-dependent opacity effects within this newly-emitted component and the core.

Table 5. Polynomial coefficients of the fits shown in Fig. 4: X(t)=$\sum_{n=0}^{2} A_n x_n t^n$, Y(t)=$\sum_{n=0}^{2} A_n y_n t^n$.

Component	A0	A1	A2
a X	249.91	-0.13	0
Y	-184.10	0.09	0
b X	120.16	-0.06	0
Y	-262.66	0.13	0
c X	$2.0633e+05$	-272.11	0.12
Y	$1.638e+05$	-252.98	0.13
d X	-41038	41.22	-0.01
Y	$-1.2056e+05$	120.92	-0.03
e X	-94801	95.23	-0.02
Y	$-1.1181e+05$	112.15	-0.03
f X	309.87	-0.16	0
Y	-335.75	0.17	0
g X	136.52	-0.07	0
Y	-720.33	0.36	0

3.3. Motion along bent paths

As can be seen from the maps in Fig. 1, the components seem to follow curved paths. The diversity of the individual-component paths in PKS 0528+134 is evident. Fig. 4 shows the motion of components **a**–**g** in rectangular coordinates relative to the fixed core position. We have calculated polynomial fits to the curves $X(t)$ and $Y(t)$ and list the resultant polynomial coefficients in Table 5. It is obvious that some of the components move on curved trajectories, and that these are different for each component. In Fig. 5 we plot the position angle versus the core separa-

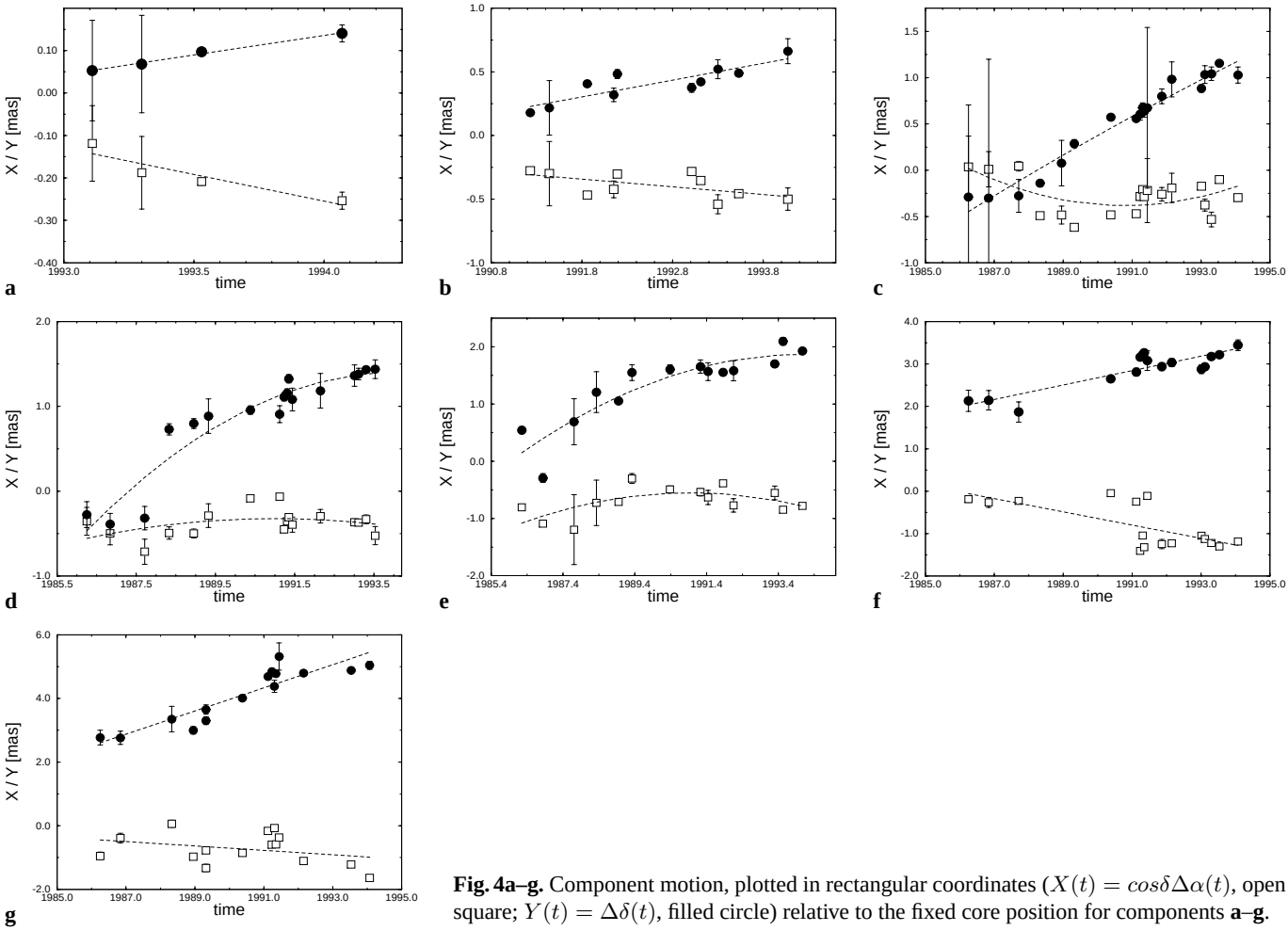

Fig. 4a–g. Component motion, plotted in rectangular coordinates ($X(t) = cos\delta\Delta\alpha(t)$, open square; $Y(t) = \Delta\delta(t)$, filled circle) relative to the fixed core position for components **a**–**g**.

Table 6. The table lists the polynomial coefficients derived from quadratic regressions performed on the data sets for components **a**–**d**.

Component	A0	A1	A2
a	44.771	255.9	−694.15
b	89.781	−137.6	96.288
c	343.04	−518.68	201.82
d	368.3	−742.91	382.49

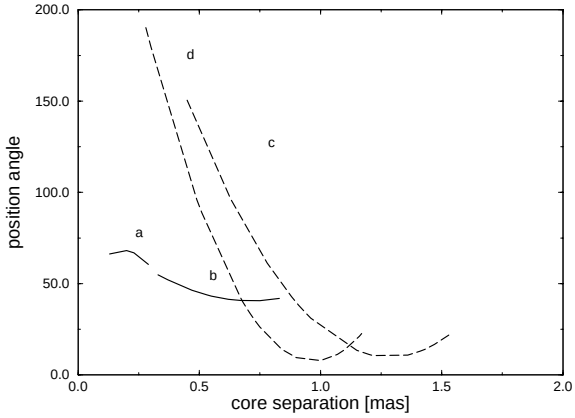

Fig. 5. Position angle versus core separation from the paths of the 4 youngest components in PKS 0528+134.

tion in order to characterize the mean trajectory for the inner jet components **a**–**d** (polynomial coefficients are given in Table 6).

From Fig. 5 it appears not only that individual component pairs **a**–**b** and **c**–**d** move on similar trajectories, but also that the ejection position angles for the two pairs are displaced by about 100 degrees. This is consistent with observations at 22 and 86 GHz (Krichbaum et al. 1995; Britzen & Krichbaum 1997) in which the most recent jet components are ejected at position angles nearly perpendicular to the jet direction at larger mas scales ($\sim$ 3 mas). The comparison of the individual component trajectories leads to the conclusion that the bending is more pronounced near the core and that the paths straighten further out. The linear fits to the component motions (see Fig. 2) give an adequate representation of the major part of the trajectories and will be used in the discussion.

4. Discussion

In the following, we place characteristics we found for PKS 0528+134 in the context of current theories. With almost 60

EGRET detections of quasars, it has become increasingly clear that gamma-ray sources are preferentially radio-bright, compact-core, flat-spectrum sources, many of which have been classified as optically violent variables (OVV) or blazars. Superluminal motion is common to all those sources studied in more detail (e.g., Barthel et al. 1995; Bower et al. 1997). Many sources also exhibit a parsec-scale jet that is bent or is misaligned with the kiloparsec-scale jet (see, e.g., Bower et al. 1997). Thus the radio properties of the AGN seem to be connected with the gamma-ray production. PKS 0528+134 is a gamma-ray source possessing many features common to this class of sources, but its unusual brightness and high degree of variability suggest that it belongs to a class of extreme gamma-ray objects. It is consequently well suited to investigate the physics of gamma-active blazars in view of a possible correlation between VLBI morphology and flux density variability across many bands.

4.1. Kinematics

Our data yield evidence for seven distinct components in the jet of PKS 0528+134. The inner five jet components separate from the core with similar velocities of $\sim 5c$ (see Table 4). These component speeds fall in a range typical of component speeds in superluminal sources (Vermeulen & Cohen 1994). The component velocities in PKS 0528+134 are also similar to those of gamma-ray blazars; superluminal motion is common to all sources with sufficient statistics. According to Bower et al. (1997) the number of EGRET sources with confirmed superluminal motion was 15. Our study of the component motion in PKS 0528+134 yields a much more detailed picture than has previously been obtained for this source. Yet velocities have already been published for a subset of jet components. Motions in the vicinity of the core ($\leq$ 0.2 mas) can be monitored and traced at much better resolution by high frequency VLBI. Krichbaum et al. (1995) reported apparent velocities of $\beta_{\rm app} \simeq 5$ for the innermost components. While observations performed once or twice a year seemed to be adequate to sample component motions in many sources, the mas-scale activity in PKS 0528+134 clearly requires a higher sampling rate. The observations of PKS 0528+134 presented here cover a long enough time span and comprise a sufficient number of epochs to accomplish this for some of the components. Morphologically, the jet is bent twice, and tracing the individual component paths leads to the conclusions that the bending is more pronounced near the core and that the paths straighten further out. Such bending on small angular scales has been observed also in many other sources and seems to be a quite common phenomenon in AGN (see, e.g., Zensus et al. 1995 for 3C345; Wagner et al. 1995 for PKS 0420-014). In addition, the components follow differently curved paths. When the components **c**–**d** were within ≤ 0.5 mas of the core, they lay at position angle of $\sim 100^\circ - 150^\circ$, but the components **a**–**b**, which are currently that close to the core, lie at position angle of $\sim 50^\circ - 80^\circ$. Thus in time, adjacent component pairs follow trajectories that are significantly displaced in position angle. Component trajectories which differ from the trajectories of their precursors have already been observed for three other sources: Zensus et al. (1995) and Krichbaum et al. (1998) discussed evidence for a similar pattern of motion in the jets of 3C345 and 3C273 respectively; Piner & Kingham (1997) presented different trajectories for different components when the components were at the same distance from the core in 1611+343.

Although the data are limited, there is some indication for an edge brightening of the jet that leads to an apparent splitting of the jet axis, (components **f** and **g**) at $\sim$ 3 mas. A broad variety of different theories have been proposed in order to explain the observed wiggling of the jet. The appearance of a curved jet could be caused by different components being ejected along different, yet straight, trajectories (i.e., ballistic motion). However, following the individual jet components of PKS 0528+134 along their curved paths shows that they are not ballistic and precession models are therefore implausible as explanations for the observed curved jet. Binary black holes (e.g., Begelman et al. 1980) or hydrodynamic instabilities (e.g., Hardee 1987) are commonly cited as the source for helical motion in jets. The resulting wiggles have a similar appearance to the wiggles caused by precession; however the origin, period, and opening angle are different (Kaastra & Roos 1992). Another alternative is that each component is following the same curved trajectory, where some force is constraining the components to follow the curved path. A number of models have been proposed to explain the curved trajectories seen in 3C 345 and similar sources based on helical motion (Camenzind & Krockenberger 1992; Hardee 1987; Qian et al. 1991, 1996). No clear case can be made for one particular helical model to explain the observed curvature and variety of the different paths in PKS 0528+134, although Kelvin-Helmholtz instabilities can account for the edge brightening.

4.2. Correlations between component ejections and gamma-flares

Our data yield evidence for a correlation between the instances of component ejection and the beginning of phases of enhanced flux density activity in the radio bands (ejection of **c**–**d**) and radio- and gamma-bands (ejection of **a**–**b**). This sequence of ejection of VLBI components from the core following a high-energy outburst, that in turn could then be traced through to lower energy bands, conforms with observations for some other sources: see, e.g., Krichbaum et al. 1995 (3C 454.3), Wagner et al. 1995 (PKS 0420-014), Bower et al. 1997 (NRAO 530), Piner & Kingham 1997 (1611+343), Krichbaum et al. 1998 (3C 273) and Unwin et al. 1998 (3C 279). Whereas the pair of components **c** and **d** could be related to the maximum in the light-curve near 1986, the pair of younger components **a** and **b** might relate to the beginning of two secondary outbursts peaking in $\sim$ 1993.6 and 1994.6. These secondary flares were accompanied by a major outburst in gamma-rays peaking in March 1993 (Mukherjee et al. 1996) and preceded a major radio outburst in 1996.6. The main difference between the components preceding radio or radio- and gamma-flares is the position angle, which might indicate that the ejection direction correlates with

the strength of the radio flares. This has to be confirmed by future higher dynamic-range VLBI observations. The study of the correlation between the ejection of VLBI components and the evolution of broad band gamma-optical-radio flares can test the high energy emission mechanisms in the innermost regions of blazar jets (Marscher 1995; Marscher & Travis 1996). Previous studies have taken the gamma-ray emission mechanism to be either the synchrotron self-Compton (SSC) process or the inverse Compton (IC) process on an external radiation field (Dermer et al. 1992; Marashi et al. 1992; Blandford 1993; Sikora et al. 1994; Dermer & Schlickeiser 1994; Blandford & Lenvinson 1995; Bloom & Marscher 1993, 1996), although there are also other models (see, e.g., Bednarek 1993; Mannheim 1993). The flux of the inverse-Compton gamma-rays should be more-or-less correlated with the radio flux, so such a correlation is a necessary test for this mechanism. Various papers have investigated this possibility observationally (see, e.g., Valtaoja & Teraesranta 1995; Reich et al. 1993; Mücke et al. 1997; Bower et al. 1997); but since gamma-flares appear to be of very short duration, it is very difficult to link these events directly by observations. Comparisons between individual gamma-ray and radio-wave flares are hampered because of poor sampling and the highly variable character of blazars at all wavelengths. VLBI might not be the optimal tool to investigate this correlation, as even higher frequency VLBI observations and closer time sampling are necessary.

Our data nevertheless allow the following conclusions. The 1991.5 gamma-event occurred near the minimum of the mm-light-curve. Based on this observation we conclude that the associated mm-radio outburst may be a delayed counterpart of the gamma-ray event. The mm-radio outburst shows the typical 3-stage spectral evolution from higher to lower frequency. The multi-frequency evolution behaviour of this outburst can be fitted by the "burst injection model" (Qian et al. 1996, 1998a) for 10 frequencies from ~ 150 GHz to 2.3 GHz. In contrast to the 1991.5 gamma-event, the 1993.23 high-amplitude gamma-ray flare occurred close before the maximum of a months-long millimeter flare. According to Zhang et al. (1994), this is characteristic of the non-linear SSC effect. However, PKS 0528+134 is a low-polarization quasar with a large ratio of Compton to synchrotron luminosity, so the gamma-ray flares in this source may be due to external Compton scattering (Ghisellini 1997; Qian et al. 1998b). Therefore the simultaneity of the gamma- and mm-outbursts needs further investigation. VLBI measurements show that the superluminal knots in this source are ejected close to the times when gamma-events occur. According to this observation, mm-outbursts should be delayed relative to gamma-events (but see Bower et al. 1997). Based on an external Compton scattering model, Qian et al. (1998b, 1998c) investigated the evolutionary relationship between the gamma-ray flares and mm-outbursts in PKS 0528+134. It is shown that the spectral tracks of the mm-outburst do not directly connect to the spectral turnover of the synchrotron spectra associated with the gamma-flares. The physical processes relevant to the gamma-ray/radio correlation have to be clarified by the help of future observations. A confirmation of the delay of mm-radio outbursts relative to gamma-ray flares in this source might be expected.

5. Conclusions

We present twenty 8.4 GHz VLBI observations of PKS 0528+134 that cover a period of almost eight years (1986.25 to 1994.07). The jet can be well described by seven distinct jet components. We have detected apparent superluminal motion for at least five components. We portray the component trajectories and extrapolate them back to the time of component ejection. We find that the times of ejection agree well with the beginning of phases of enhanced flux-density activity for four components. The component pair **c**–**d** can be linked to the start of the flare in 1986 and the pair **a**–**b** to the beginning of two secondary flares which were accompanied by a gamma-ray flare. The jet of PKS 0528+134 is bent twice and the detailed study of individual component trajectories reveals the existence of different paths. Pairs of components follow similar-looking trajectories, but ones displaced from each other in position angle. We speculate about a possible correlation between the direction of ejection from the core and the strength of the correlated radio outburst.

Acknowledgements. The authors thank A.P. Marscher for useful discussions. This research has made use of data from the University of Michigan Radio Astronomy Observatory which is supported by the National Science Foundation and by funds from the University of Michigan. We thank M. and H. Aller for communicating data prior to publication. We also thank A.M. Gontier, C. Schalinski and K. Standke for helpful comments and A. Mueskens for help exporting the VLBI data. Part of this work was supported by the European Commission, TMR Programme, Research Network Contract ERBFMRXCT97-0034 CERES.

References

Alberdi A., Marcaide J.M., Marscher A.P., et al., 1993, ApJ 402, 160
Aller H.D., Aller M.F., Latimer G.E., Hodge P.E., 1985, ApJS 59, 513
Aller H.D., Aller M.F., 1996, A&AS 189, 9902
Barthel P.D., Conway J.E., Myers S.T., Pearson T.J., Readhead A.C.S., 1995, ApJ 444, 21
Bednarek W., 1993, ApJ 402, L29
Begelman M.C., Blandford R.D., Rees M.J., 1980, Nat 287, 307
Blandford R.D., 1993, In: Friedlander M., Gehrels N., Macomb D.J. (eds.) AIP Conf. Proc. 280, Compton Gamma-Ray Observatory, AIP, New York, 533
Blandford R.D., Lenvinson A., 1995, ApJ 441, 79
Bloom S.D., Marscher, A.P., 1993, In: Friedlander M., Gehrels N., Macomb D.J. (eds.) AIP Conf. Proc. 280, Compton Gamma-Ray Observatory, AIP, New York, 578
Bloom S.D., Marscher A.P., 1996, ApJ 461, 657
Bower G.C., Backer D.C., Wright M., et al., 1997, ApJ 484, 118
Britzen S., Krichbaum T.P., 1997, In: Proceedings of the 3rd EVN/JIVE VLBI Symposium. Vistas in Astronomy 41, 275
Britzen S., Witzel A., Krichbaum T.P., 1996, In: Kirk J.G., von Montigny C., Camenzind M., Wagner S. (eds.) Proceedings of the Heidelberg Workshop on Gamma-ray Emitting AGNs. Max-Planck-Inst. Kernphys., Heidelberg, 109

Britzen S., Witzel A., Krichbaum T.P., Roland J., Wagner S., 1998, In: Zensus J.A., Taylor G.B., Wrobel J.M. (eds.) IAU Colloquium 164. ASP Conf. Ser. 144, 43
Camenzind M., Krockenberger M., 1992, A&A 255, 59
Carter W.E., Robertson D.S., 1984, In: International Symposium on Space Techniques for Geodynamics Volume 1 (A86-29426 12-46). Sopron, Hungary, Magyar Tudomanyos Akademia Geodeziai es Geofizikai Kutato Intezet, 1984, 214-222
Carter W.E., Robertson D.S., Nothnagel A., Nicolson G.D., Schuh H., 1988, JGR 93, 14947
Charlot P., 1990, A&A 229, 51
Charlot P., 1992, JAF 43, 39
Cohen M.H., Moffet A.T., Schilizzi R.T., et al., 1975, ApJ 201, 249
Condon J.J., Hicks P.D., Jauncey D.L., 1977, AJ 82, 692
Dermer C.D., Schlickeiser R., 1994, ApJS 90, 945
Dermer C.D., Schlickeiser R., Mastichiadis A., 1992, A&A 256, L27
Eckart A., Witzel A., Biermann P., Johnston K.J., et al., 1986, A&A 168, 17
Fichtel C.E., Bertsch D.L., Dingus B.L., et al., 1994, ApJ 434, 557
Fugmann W., Meisenheimer K., 1988, A&AS 76, 145
Ghisellini G., 1997, In: Ostrowski M., Sikora M., Madejski G., Begelman M. (eds.) Relativistic Jets in AGNs. Proc. of the International Conference, Cracow, Poland, 262
Hardee P.E., 1987, ApJ 318, 78
Hunter S.D., Bertsch D.L., Dingus B.L., et al., 1993, ApJ 409, 134
Kaastra J.S., Roos N., 1992, A&A 254, 96-98
Krichbaum T.P., Britzen S., Standke K.J., Witzel A., Zensus J.A., 1995, In: Cohen M., Kellermann K.I. (eds.) Quasars and AGN: High Resolution Radio Imaging. Proc. Nat. Acad. Sci., USA 92, 11377
Krichbaum T.P., Kraus A., Otterbein K., et al., 1998, In: Zensus J.A., Taylor G.B., Wrobel J.M. (eds.) IAU Colloquium 164. ASP Conf. Ser. 144, 37
Kühr H., Witzel A., Pauliny-Toth I.I.K., Nauber U., 1981, A&AS 45, 367
Mannheim K., 1993, A&A 269, 67
Maraschi L., Ghisellini G., Celotti A., 1992, ApJ 397, L5
Marcaide J.M., Alberdi A., Elosegui P., et al., 1989, A&A 211, 23
Marscher, A.P., 1995, Proc. Natl. Acad. Sci., USA 92, 11439
Marscher, A.P., Travis, J.P., 1996, A&AS 120, 537
McNaron-Brown K., Johnson W.N., Jung G.V., et al., 1995, ApJ 451, 575
von Montigny C., Bertsch D.L., Chiang J., et al., 1995, ApJ 440, 525
Mücke A., Pohl M., Reich P., et al., 1997, A&A 320, 33
Mukherjee R., Dingus B.L., Gear W.K., et al., 1996, ApJ 470, 831
Piner B.G., Kingham K., 1997, ApJ 479, 684-693
Pohl M., Reich W., Krichbaum T., et al., 1995, A&A 303, 383
Pohl M., Reich W., Schlickeiser R., Ungerechts H., 1996, A&AS 120, 529
Qian S.J., Krichbaum T.P., Witzel A., et al., 1991, Acta Astron. Sin. 32, 369, Transl. Chin. Astron. Astrophys. 16, 137
Qian S.J., Witzel A., Britzen S., Krichbaum T.P., Kraus A., 1996, In: Hardee P.E., Bridle A.H., Zensus J.A. (eds.) Energy Transport in Radio Galaxies and Quasars. ASP Conf. Ser. 100, 61
Qian S.J., Britzen S., Witzel A., 1998a, Acta Astrophys. Sin. 18, 179
Qian S.J., Zhang X.Z., Witzel A., et al., 1998b, In: Zensus J.A., Taylor G.B., Wrobel J.M. (eds.) IAU Colloquium 164. ASP Conf. Ser. 144, 93
Qian S.J., Britzen S., Witzel A., et al., 1998c, Acta Astrophys. Sin. 18, in press
Reich W., Steppe H., Schlickeiser R., et al., 1993, A&A 273, 65
Schalinski C.J., Alef W., Witzel A., Campbell J., Schuh H., 1988, In: The Impact of VLBI on Astrophysics and Geophysics. Proc. of the IAU Symp. No. 129, Cambridge, MA, USA, 359
Sikora M., Begelman M.C., Rees M.J., 1994, ApJ 432, 606
Sreekumar P., Dingus B.L., Bertsch D.L., et al., 1993, IAU Circ. 5753
Sreekumar P., Bertsch D.L., Dingus B.L., et al., 1996, ApJ 464, 628
Stevens J.A., Litchfield S.J., Robson E.I., et al., 1994, ApJ 437, 91
Tang G.Q., Ronnang B., Baath L., 1987, A&A 185, 87
Tang G.Q., Ronnang B., 1988, In: Reid M.J., Moran J.M. (eds.) The impact of VLBI on astrophysics and geophysics. Proceedings of the 129th IAU symposium, Cambridge, MA, 431
Tang G.Q., Ronnang B., Baath L., 1989, A&A 216, 31
Thompson D.J., Bertsch D.L., Dingus B.L., et al., 1995, ApJS 101, 259
Valtaoja E., Teraesranta H., 1995, A&A 297, L13
Valtaoja E., Teraesranta H., 1996, ApJS 120, 491
Vermeulen R.C., Cohen M.H., 1994, ApJ 430, 467
Vicente L., Charlot B., Sol H., 1996, A&A 312, 727
Wagner S.J., Camenzind M., Dreissigacker O., et al., 1995, A&A 298, 688
Wall J.V., Peacock J.A., 1985, MNRAS 216, 173
Unwin S.C., Wehrle A.E., Xu W., Zook A.C., Marscher A.P., 1998 In: Zensus J.A., Taylor G.B., Wrobel J.M. (eds.) IAU Colloquium 164. ASP Conf. Ser. 144, 69
Witzel A., Schalinski C.J., Johnston K.J., et al., 1988, A&A 206, 245
Zensus J.A., Cohen M.H., Unwin S.C., 1995, ApJ 443, 35
Zhang Y.F., Marscher A.P., Aller H.D., et al., 1994, ApJ 432, 91